

INCREASING EVIDENCE FOR HEMISPHERICAL POWER ASYMMETRY IN THE FIVE-YEAR WMAP DATA

J. HOFTUFT¹, H. K. ERIKSEN^{1,2}, A. J. BANDAY^{3,4}, K. M. GÓRSKI^{5,6,7}, F. K. HANSEN¹ AND P. B. LILJE^{1,2}

Draft version November 4, 2021

ABSTRACT

Motivated by the recent results of Hansen et al. (2008) concerning a noticeable hemispherical power asymmetry in the WMAP data on small angular scales, we revisit the dipole modulated signal model introduced by Gordon et al. (2005). This model assumes that the true CMB signal consists of a Gaussian isotropic random field modulated by a dipole, and is characterized by an overall modulation amplitude, A , and a preferred direction, \hat{p} . Previous analyses of this model has been restricted to very low resolution (ie., 3.6° pixels, a smoothing scale of 9° FWHM and $\ell \lesssim 40$) due to computational cost. In this paper, we double the angular resolution (ie., 1.8° pixels and 4.5° FWHM smoothing scale), and compute the full corresponding posterior distribution for the 5-year WMAP data. The results from our analysis are the following: The best-fit modulation amplitude for $\ell \leq 64$ and the ILC data with the WMAP KQ85 sky cut is $A = 0.072 \pm 0.022$, non-zero at 3.3σ , and the preferred direction points toward Galactic coordinates $(l, b) = (224^\circ, -22^\circ) \pm 24^\circ$. The corresponding results for $\ell \lesssim 40$ from earlier analyses was $A = 0.11 \pm 0.04$ and $(l, b) = (225^\circ, -27^\circ)$. The statistical significance of a non-zero amplitude thus increases from 2.8σ to 3.3σ when increasing ℓ_{\max} from 40 to 64, and all results are consistent to within 1σ . Similarly, the Bayesian log-evidence difference with respect to the isotropic model increases from $\Delta \ln E = 1.8$ to $\Delta \ln E = 2.6$, ranking as “strong evidence” on the Jeffreys’ scale. The raw best-fit log-likelihood difference increases from $\Delta \ln \mathcal{L} = 6.1$ to $\Delta \ln \mathcal{L} = 7.3$. Similar, and often slightly stronger, results are found for other data combinations. Thus, we find that the evidence for a dipole power distribution in the WMAP data increases with ℓ in the 5-year WMAP data set, in agreement with the reports of Hansen et al. (2008).

Subject headings: cosmic microwave background — cosmology: observations — methods: statistical

1. INTRODUCTION

The question of statistical isotropy in the cosmic microwave background (CMB) has received much attention within the cosmological community ever since the release of the first-year Wilkinson Microwave Anisotropy Probe (WMAP; Bennett et al. 2003a) in 2003. The reasons for this are two-fold. On the one hand, the current cosmological concordance model is based on the concept of inflation (Starobinsky 1980; Guth et al 1981; Linde et al. 1982; Mukhanov et al. 1981; Starobinsky et al 1982; Linde et al. 1983, 1994; Smoot et al. 1992; Ruhl et al 2003; Rynyan et al. 2003; Scott et al. 2003), which predicts a statistically homogeneous and isotropic universe. Since inflation has proved highly successful in describing a host of cosmological probes, most importantly the CMB and large-scale power spectra, this undeniably imposes a strong theoretical prior towards isotropy and homogeneity.

On the other hand, many detailed studies of the WMAP sky maps, employing higher-order statistics,

have revealed strong hints of both violation of statistical isotropy and non-Gaussianity. Some early notable examples include unexpected low- ℓ correlations (de Oliveira-Costa et al. 2004), a peculiar large cold spot in the southern Galactic hemisphere (Vielva et al. 2004), and a dipolar distribution of large-scale power (Eriksen et al. 2004a). Today, the literature on non-Gaussianity and violation of statistical isotropy in the WMAP data has grown very large, indeed (e.g., Bernui et al. 2006; Bielewicz et al. 2005; Copi et al. 2006; Cruz et al. 2005, 2006; Eriksen et al. 2004b,c, 2005; Jaffe et al. 2005, 2006; Martínez-González et al. 2006; McEwen et al. 2008; Räth et al. 2007; Yadav & Wandelt 2008), and it would be unwise not to consider these issues very seriously.

Of particular interest to us is the question of hemispherical distribution of power in the WMAP data, first reported by Eriksen et al. (2004a) and later confirmed by, e.g., Hansen et al. (2004) and Eriksen et al. (2005). The most recent works on this topic include those presented by Hansen et al. (2008), who found that the power asymmetry extends to much smaller scales than previously thought, and by Eriksen et al. (2007b), who quantified the large-scale power asymmetry in the 3-year WMAP data using an optimal Bayesian framework.

A separate, but possibly physically related, line of work was recently presented by Groeneboom & Eriksen (2009), who considered the specific model for violation of Lorenz invariance in the early universe, proposed by Ackerman et al. (2007). This model involves CMB correlations with a quadrupolar distribution on the sky, and is thus orthogonal to the current dipolar

Electronic address: h.k.k.eriksen@astro.uio.no

¹ Institute of Theoretical Astrophysics, University of Oslo, P.O. Box 1029 Blindern, N-0315 Oslo, Norway

² Centre of Mathematics for Applications, University of Oslo, P.O. Box 1053 Blindern, N-0316 Oslo, Norway

³ Centre d’Etude Spatiale des Rayonnements, 9, av du Colonel Roche, BP 44346, 31028 Toulouse Cedex 4, France

⁴ Max-Planck-Institut für Astrophysik, Karl-Schwarzschild-Str. 1, Postfach 1317, D-85741 Garching bei München, Germany

⁵ Jet Propulsion Laboratory, 4800 Oak Grove Drive, Pasadena CA 91109

⁶ California Institute of Technology, Pasadena, CA 91125

⁷ Warsaw University Observatory, Aleje Ujazdowskie 4, 00-478 Warszawa, Poland

model. Surprisingly, when analyzing the 5-year WMAP data, Groeneboom & Eriksen (2009) found supportive evidence for this model at the 3.8σ significance level, when considering angular scales up to $\ell \leq 400$. Thus, assuming that the WMAP observations are free of unknown systematics, there appears to be increasing evidence for both dipolar and quadrupolar structure in the CMB power distribution, at all angular scales.

In this paper, we repeat the Bayesian analysis of Eriksen et al. (2007b), but double the angular resolution of the data. Nevertheless, we are still limited to relatively low angular resolutions, since the method inherently relies on brute-force evaluation of a pixel-based likelihood, and therefore scales as $\mathcal{O}(N_{\text{pix}}^3)$. Yet, simply by spending more computer resources we are able to increase the pixel resolution from $N_{\text{side}} = 16$ to 32 and decrease the degradation smoothing scale from 9° to 4.5° FWHM. This provides additional support for multipoles between $\ell \approx 40$ and 80. While not sufficient to provide a full and direct comparison with the results of Hansen et al. (2008), it is a significant improvement over the results presented by Eriksen et al. (2007b).

2. OVERVIEW OF MODEL AND ALGORITHMS

The Bayesian analysis framework used in this paper are very similar to that employed by Eriksen et al. (2007b). We therefore only give a brief overview of its main features here, and refer the reader interested in the full details to the original paper and references therein.

2.1. Data model and likelihood

The starting point for our analysis is the phenomenological CMB signal model first proposed by Gordon et al. (2005),

$$\mathbf{d}(\hat{n}) = [1 + f(\hat{n})]\mathbf{s}(\hat{n}) + \mathbf{n}(\hat{n}). \quad (1)$$

Here $\mathbf{d}(\hat{n})$ denotes the observed data in direction \hat{n} , $\mathbf{s}(\hat{n})$ is an intrinsically isotropic and Gaussian random field with power spectrum C_ℓ , $f(\hat{n})$ is an auxiliary modulating field, and $\mathbf{n}(\hat{n})$ denotes instrumental noise.

Obviously, if $f = 0$, one recovers the standard isotropic model. However, we are interested in a possible hemispherical asymmetry, and we therefore parametrize the modulation field in terms of a dipole with a free amplitude A and a preferred direction \hat{p} ,

$$f(\hat{n}) = A(\hat{n} \cdot \hat{p}). \quad (2)$$

The modulated signal component is thus an anisotropic, but still Gaussian, random field, with covariance matrix

$$\mathbf{S}_{\text{mod}}(\hat{n}, \hat{m}) = [1 + A(\hat{n} \cdot \hat{p})]\mathbf{S}_{\text{iso}}(\hat{n}, \hat{m})[1 + A(\hat{m} \cdot \hat{p})], \quad (3)$$

where

$$\mathbf{S}_{\text{iso}}(\hat{n}, \hat{m}) = \frac{1}{4\pi} \sum_{\ell} (2\ell + 1) C_\ell P_\ell(\hat{n} \cdot \hat{m}). \quad (4)$$

We now introduce one new feature compared to the analysis of Eriksen et al. (2007b), for two reasons. First, we are interested in studying the behaviour of the modulation field as a function of ℓ -range, and therefore want a mechanism to restrict the impact of the modulation parameters in harmonic space. Second, we also want to minimize the impact of the arbitrary regularization noise (see Section 3) on the modulation parameters at high ℓ 's.

Therefore, we split the signal covariance matrix into two parts, one modulated low- ℓ part and one isotropic high- ℓ part,

$$\mathbf{S}_{\text{total}} = \mathbf{S}_{\text{mod}} + \mathbf{S}_{\text{iso}}, \quad (5)$$

where only multipoles between $2 \leq \ell < \ell_{\text{mod}}$ are included in \mathbf{S}_{mod} , and only multipoles at $\ell \geq \ell_{\text{mod}}$ are included in \mathbf{S}_{iso} . (Note that we are not proposing a physical mechanism for generating the modulation field in this paper, but only attempt to characterize its properties. This split may or may not be physically well-motivated, but it does serve a useful purpose in the present paper as it allows us to study the scale dependence of the modulation field in a controlled manner.)

Including instrumental noise and possible foreground contamination, the full data covariance matrix reads

$$\mathbf{C} = \mathbf{S}_{\text{mod}}(A, \hat{p}) + \mathbf{S}_{\text{iso}} + \mathbf{N} + \mathbf{F}. \quad (6)$$

The noise and foreground covariance matrices depend on the data processing, and will be described in greater detail in §3.

We also have to parametrize the power spectrum for the underlying isotropic component, C_ℓ . Following Eriksen et al. (2007b), we choose a simple two-parameter model with a free amplitude q and tilt n for this purpose,

$$C_\ell = q \left(\frac{\ell}{\ell_0} \right)^n C_\ell^{\text{fid}}. \quad (7)$$

Here ℓ_0 is a pivot multipole and C_ℓ^{fid} is a fiducial model, in the following chosen to be the best-fit Λ CDM power law spectrum of Komatsu et al. (2009).

Since both the signal and noise are assumed to be Gaussian, the log-likelihood now reads

$$-2 \log \mathcal{L}(A, \hat{p}, q, n) = \mathbf{d}^T \mathbf{C}^{-1} \mathbf{d} + \log |\mathbf{C}|, \quad (8)$$

up to an irrelevant constant, with $\mathbf{C} = \mathbf{C}(A, \hat{p}, q, n)$.

2.2. The posterior distribution and Bayesian evidence

The posterior distribution for our model is given by Bayes' theorem,

$$P(q, n, A, \hat{p} | \mathbf{d}, H) = \frac{\mathcal{L}(q, n, A, \hat{p}) P(q, n, A, \hat{p} | H)}{P(\mathbf{d} | H)}. \quad (9)$$

Here $P(q, n, A, \hat{p} | H)$ is a prior, and $P(\mathbf{d} | H)$ is a normalization factor often called the ‘‘Bayesian evidence’’. Note that we now have included an explicit reference to the hypothesis (or model), H , in all factors, as we will in the following compare two different hypotheses, namely ‘‘H1: The universe is isotropic ($A = 0$)’’ versus ‘‘H2: The universe is anisotropic ($A \neq 0$)’’.

We adopt uniform priors for all priors in the following. Specifically, we adopt $P(q) = \text{Uniform}[0.5, 1.5]$ and $P(n) = \text{Uniform}[-0.5, 0.5]$ for the power spectrum, and a uniform prior over the sphere for the preferred axis, \hat{p} . The modulation amplitude prior is chosen uniform over $[0, A_{\text{max}}]$, where $A_{\text{max}} = 0.15$ is sufficiently large to fully encompass the non-zero parts of the likelihood. If more liberal priors are desired, the interested reader can easily calculate the corresponding evidence by subtracting the logarithm of the volume expansion factor from the results quoted in this paper.

With these definitions and priors, the posterior distribution, $P(q, n, A, \hat{\mathbf{p}}|\mathbf{d}, H)$ is mapped out with a standard MCMC sampler. The Bayesian evidence, $E = P(\mathbf{d}|H)$ is computed with the “nested sampling” algorithm (Skilling 2004; Mukherjee et al. 2006). For further details on both procedures, we refer the interested reader to Eriksen et al. (2007b).

For easy reference, we recall Jeffreys’ interpretational scale for the Bayesian evidence (Jeffreys 1961): A value of $\Delta \ln E < 1$ indicates a result “not worth more than a bare mentioning”; a value of $1 < \Delta \ln E < 2.5$ is considered as “significant” evidence; a value of $2.5 < \Delta \ln E < 5$ is considered “strong to very strong”; and $\Delta \ln E > 5$ ranks as “decisive”.

3. DATA

In this paper we analyze several downgraded versions of the five-year WMAP temperature sky maps, namely the template-corrected Q -, V - and W -band maps, as well as the “foreground cleaned” Internal Linear Combination (ILC) map (Gold et al. 2009). Each map is downgraded to low resolution as follows (Eriksen et al. 2007a): First, each map is downgraded to a HEALPix⁸ resolution of $N_{\text{side}} = 32$, by smoothing to an effective resolution of 4.5° FWHM and properly taking into account the respective pixel windows. We then add uniform Gaussian noise of $\sigma_n = 1 \mu\text{K}$ RMS to each pixel, in order to regularize the pixel-pixel covariance matrix at small angular scales. The resulting maps have a signal-to-noise ratio of unity at $\ell = 80$, and are strongly noise dominated at $\ell_{\text{max}} = 95$.

Two different sky cuts are used in the analyses, both of which are based on the WMAP KQ85 mask (Gold et al. 2009). In the first case, we directly downgrade the KQ85 cut to the appropriate N_{side} , by excluding any HEALPix pixel for which more than half of the corresponding sub-pixels are missing. This mask is simply denoted KQ85. In the second case, we smooth the mask image (consisting of 0’s and 1’s) with a beam of 4.5° FWHM, and reject all pixels with a value less than 0.99. We call this expanded mask KQ85e. The two mask remove 16.3% and 26.9% of the pixels, respectively.

The instrumental signal-to-noise ratio of the WMAP data is very high at large angular scales, at about 150 for the V -band at $\ell = 100$. The only important noise contribution in the downgraded sky maps is therefore the uniform regularization noise, which is not subject to the additional beam smoothing. We therefore approximate the noise covariance matrix by $N_{ij} = \sigma_n^2 \delta_{ij}$. Note that this approximation was explicitly validated by Eriksen et al. (2007b) for the 3-year WMAP data, which have higher instrumental noise than the 5-year data.

We also marginalize over a fixed set of “foreground templates”, \mathbf{t}_i , by adding an additional term to the data covariance matrix on the form $\mathbf{F}_i = \alpha_i \mathbf{t}_i \mathbf{t}_i^T$, with $\alpha_i \gtrsim 10^3$, for each template. In addition to one monopole and three dipole templates⁹, we use the V -ILC difference map as a template for both the V -band and ILC maps, the Q -ILC difference for the Q -band, and the W -ILC difference for the W -band. However, these foreground

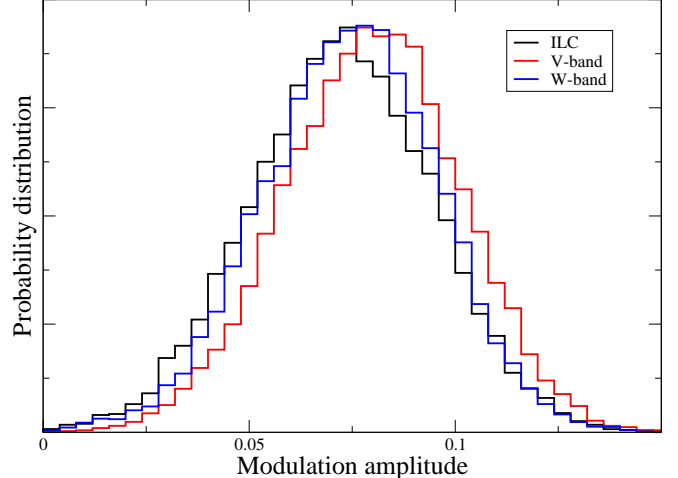


FIG. 1.— Posterior distributions for the dipole modulation amplitude, marginalized over direction and CMB power spectrum, computed for the KQ85 sky cut and $\ell_{\text{mod}} = 64$.

templates do not affect the results noticeably in either case, due to the sky cuts used.

4. RESULTS

The main results from the analysis outlined above are summarized in Table 1. We consider nine different data combinations (ie., frequency bands, masks and multipole range), and show 1) the best-fit modulation axis and amplitude, both with 68% confidence regions; 2) the statistical significance of the corresponding amplitude (ie., A/σ_A); and 3) the raw improvement in χ^2 and Bayesian log-evidence for the modulated model over the isotropic model. The last items are shown for the ILC with the KQ85 sky cut only. For reference, we also quote the ILC result for the Kp2 mask (Bennett et al. 2003b) reported by Eriksen et al. (2007b) when analysing the $N_{\text{side}} = 16$ and 9° FWHM data.

The reason for providing the full evidence for only one data set is solely computational. The total CPU cost for the full set of computations presented here was $\sim 50\,000$ CPU hours, and the evidence calculation constitutes a significant fraction of this. On the other hand, the evidence is closely related to the significance level A/σ_A , and one can therefore estimate the evidence level for other cases in Table 1 given the two explicit evidence values and significances. We have therefore chosen to spend our available CPU time on more MCMC posterior analyses, rather than on more evidence computations.

We consider first the results for the ILC map with the KQ85 mask and $\ell_{\text{mod}} = 64$. In this case, the best-fit amplitude is $A = 0.073 \pm 0.022$, non-zero at the 3.3σ confidence level. The best-fit axis points towards Galactic coordinates $(l, b) = (224^\circ, -22^\circ)$, with a 68% uncertainty of 24° . These results are consistent with the results presented by Eriksen et al. (2007b), who found an amplitude of $A = 0.11 \pm 0.04$ and a best-fit axis of $(l, b) = (225^\circ, -27^\circ)$ for $\ell \lesssim 40$.

Second, we see that these results are only weakly dependent on frequency, as both the V -band and W -band for the same mask and ℓ -range have amplitudes within 0.5σ of the ILC map, with $A = 0.080$ and $A = 0.074$ and non-zero at 3.8σ and 3.5σ , respectively. (We have not included the Q -band analysis for the KQ85 mask, as there

⁸ <http://healpix.jpl.nasa.gov>

⁹ For an explicit demonstration of the importance of monopole and dipole marginalization on this specific problem, see Gordon 2007a

TABLE 1
SUMMARY STATISTICS FOR MODULATED CMB MODEL POSTERiors

Data	Mask	ℓ_{mod}	$(l_{\text{bf}}, b_{\text{bf}})$	A_{bf}	Significance (σ)	$\Delta \log \mathcal{L}$	$\Delta \log E$
ILC	KQ85	64	$(224^\circ, -22^\circ) \pm 24^\circ$	0.072 ± 0.022	3.3	7.3	2.6
V-band	KQ85	64	$(232^\circ, -22^\circ) \pm 23^\circ$	0.080 ± 0.021	3.8
V-band	KQ85	40	$(224^\circ, -22^\circ) \pm 24^\circ$	0.119 ± 0.034	3.5
V-band	KQ85	80	$(235^\circ, -17^\circ) \pm 22^\circ$	0.070 ± 0.019	3.7
W-band	KQ85	64	$(232^\circ, -22^\circ) \pm 24^\circ$	0.074 ± 0.021	3.5
ILC	KQ85e	64	$(215^\circ, -19^\circ) \pm 28^\circ$	0.066 ± 0.025	2.6
Q-band	KQ85e	64	$(245^\circ, -21^\circ) \pm 23^\circ$	0.088 ± 0.022	3.9
V-band	KQ85e	64	$(228^\circ, -18^\circ) \pm 28^\circ$	0.067 ± 0.025	2.7
W-band	KQ85e	64	$(226^\circ, -19^\circ) \pm 31^\circ$	0.061 ± 0.025	2.5
ILC ^a	Kp2	~ 40	$(225^\circ, -27^\circ)$	0.11 ± 0.04	2.8	6.1	1.8

NOTE. — Listed quantities are (*first column*) data set (*first column*); mask (*second column*); maximum multipole used for modulation covariance matrix, ℓ_{mod} (*third column*); marginal best-fit dipole axis (*fourth column*) and amplitude (*fifth column*) with 68% confidence regions indicated; statistical significance of non-zero detection of A (*sixth column*); the change in maximum likelihood between modulated and isotropic models, $\Delta \log \mathcal{L} = \log \mathcal{L}_{\text{mod}} - \log \mathcal{L}_{\text{iso}}$ (*seventh column*); and the Bayesian evidence difference, $\Delta \log E = \log E_{\text{mod}} - \log E_{\text{iso}}$ (*eighth column*). The latter two were only computed for one data set, due to a high computational cost. However, other values can be estimated by comparing the significances indicated in the sixth column.

^a Results computed from $N_{\text{side}} = 16$ and 9° FWHM data, as presented by Eriksen et al. (2007b).

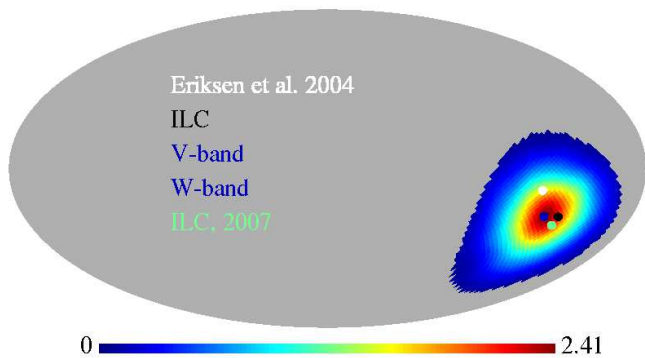


FIG. 2.— Posterior distribution for the dipole modulation axis, shown for the V-band map and KQ85 sky cut, marginalized over power spectrum and amplitude parameters. Grey sky pixels indicate pixels outside the 2σ confidence region. The dots indicate the axis 1) reported by Eriksen et al. (2004a) in white; 2) for both the ILC and V-band maps (these have the same best-fit axis) with the KQ85 sky cut in black; 3) for the W-bands in blue, and the axis reported by Eriksen et al. (2007b) in green. Note that the background distribution has been smoothed for plotting purposes to reduce visual Monte Carlo noise.

were clearly visible foreground residuals outside the mask for this case.) The corresponding marginal posteriors are shown in Figure 1, clearly demonstrating the consistency between data sets. Figure 2 compares the best-fit axes of the three data sets, and also indicates the axes reported by Eriksen et al. (2004a) and Eriksen et al. (2007b).

Next, we also see that the results are not strongly dependent on the choice of mask, as the amplitudes for the extended KQ85e mask are consistent with the KQ85 results, even though it removes an additional 10% of the sky. However, we do see, as expected, that the error bars increase somewhat by removing the additional part of the sky, and this reduces the absolute significances somewhat.

Finally, the best-fit modulation amplitudes for the V-band data and KQ85 mask are $A = 0.11$ for $\ell_{\text{mod}} = 40$, $A = 0.075$ for $\ell_{\text{mod}} = 64$ and $A = 0.066$ for $\ell_{\text{mod}} = 80$ at 3.5σ , 3.8σ and 3.7σ , respectively. This is an interesting observation for theoreticians who are interested in constructing a fundamental model for the effect: Taken at

face value, these amplitudes could indicate a non-scale invariant behaviour of A , as also noted by Hansen et al. (2008). On the other hand, the statistical significance of this statement is so far quite low, as a single common value $A \sim 0.07$ is also consistent with all measurements. Better measurements at higher ℓ 's are required to unambiguously settle this question.

5. CONCLUSIONS

Shortly following the release of the first-year WMAP data in 2003, Eriksen et al. (2004b) presented the early evidence for a dipolar distribution of power in the CMB temperature anisotropy sky, considering only the large angular scales of the WMAP data. Next, Groeneboom & Eriksen (2009) presented the evidence for a quadrupolar distribution of CMB power, and found that this feature extended over all ℓ 's under consideration. Finally, Hansen et al. (2008) found that the dipolar CMB power distribution is present also at high ℓ 's. The evidence for violation of statistical isotropy in the CMB field is currently increasing rapidly, and the significance of these detections are approaching 4σ .

In this paper, we revisit the high- ℓ claims of Hansen et al. (2008), by applying an optimal Bayesian framework based on a parametric modulated CMB model to the WMAP data at higher multipoles than previously considered with this method, albeit lower than those considered by Hansen et al. (2008). In doing so, we find results very consistent with those presented by Hansen et al. (2008): The evidence for a dipolar distribution of power in the WMAP data increases with ℓ . For example, when considering the V-band data and KQ85 sky cut, the statistical significance of the modulated model increases from 3.2σ at $\ell_{\text{mod}} = 40$, to 3.8σ at $\ell_{\text{mod}} = 64$, and 3.7σ at $\ell_{\text{mod}} = 80$.

The Bayesian evidence now also ranking within the “strong to very strong” category on Jeffreys’ scale. However, it should be noted that the Bayesian evidence is by nature strongly prior dependent, and if we had chosen a prior twice as large as the one actually used, the corresponding log-evidence for the ILC map would have fallen

from $\Delta \ln E = 2.6$ to 1.7, ranking only as “substantial” evidence. For this reason, it is in many respects easier to attach a firm statistical interpretation to the posterior distribution than the Bayesian evidence.

It is interesting to note that the absolute amplitude A may show hints of decreasing with ℓ . It is premature to say whether this is due simply to a statistical fluctuation, or whether it might point toward a non-scale invariant underlying physical effect, in which case the amplitude A should be replaced with a function $A(\ell)$. Either case is currently allowed by the data.

To answer this question, and further constrain the overall model, better algorithms are required. The current approach relies on brute-force inversion of an $N_{\text{pix}} \times N_{\text{pix}}$ covariance matrix, and therefore scales as $\mathcal{O}(N_{\text{pix}}^3)$ or $\mathcal{O}(N_{\text{side}}^6)$. However, already the present analysis, performed at $N_{\text{side}} = 32$, required $\sim 50\,000$ CPU hours, and increasing N_{side} by an additional factor of two would require ~ 3 million CPU hours. More efficient algorithms are clearly needed.

To summarize, there is currently substantial evidence for both dipolar (Hansen et al. 2008 and this work) and quadrupolar power distribution (Groeneboom & Eriksen 2009) in the WMAP data, and this is seen at all probed scales. The magnitude of the dipolar mode is considerably stronger than the quadrupolar mode, as a $\sim 3.5\sigma$ significance level is reached already at $\ell \sim 64$ for the dipole, while the same significance was obtained at $\ell \sim 400$ for the quadrupole.

These observations may prove useful for theorists attempting to construct alternative models for these features, either phenomenological

or fundamental. Considerable efforts have gone towards this goal already (e.g., Ackerman et al. 2007; Böhmer & Mota 2008; Carroll et al. 2008a,b; Chang et al. 2008; Erickcek et al. 2008a,b; Gordon et al. 2005; Gümrükçüoğlu et al. 2007; Himmetoğlu et al. 2008a,b; Kahniashvili et al. 2008; Kanno et al. 2008; Koivisto & Mota 2008a,b; Pereira et al. 2007; Pitrou et al. 2008; Pullen & Kamionkowski 2007; Watanabe et al. 2009; Yokoyama & Soda 2008), but so far no fully convincing model has been established. Clearly, more work is needed on both the theoretical and observational side of this issue. Fortunately, it is now only a few years until Planck will open up a whole new window on these issues by producing high-sensitivity maps of the CMB polarization, as well as measuring the temperature fluctuations to arc-minute scales. We will then be able to measure the properties of the dipole, quadrupole and, possibly, higher-order modes of the modulation field to unprecedented accuracy.

HKE acknowledges financial support from the Research Council of Norway. The computations presented in this paper were carried out on Titan, a cluster owned and maintained by the University of Oslo and NOTUR. Some of the results in this paper have been derived using the HEALPix (Górski et al. 2005) software and analysis package. We acknowledge use of the Legacy Archive for Microwave Background Data Analysis (LAMBDA). Support for LAMBDA is provided by the NASA Office of Space Science.

REFERENCES

- Ackerman, L., Carroll, S. M., & Wise, M. B. 2007, *Phys. Rev. D*, 75, 083502
- Bennett, C. L., et al. 2003, *ApJS*, 148, 1
- Bennett, C. L., et al. 2003b, *ApJS*, 148, 97
- Bernui, A., Vilella, T., Wuensche, C. A., Leonardi, R., & Ferreira, I. 2006, *A&A*, 454, 409
- Bielewicz, P., Eriksen, H. K., Banday, A. J., Górski, K. M., & Lilje, P. B. 2005, *ApJ*, 635, 750
- Böhmer, C. G., & Mota, D. F. 2008, *Phys. Lett. B*, 663, 168
- Bridges, M., McEwen, J. D., Lasenby, A. N., & Hobson, M. P. 2006, [[astro-ph/0605325](#)]
- Carroll, S. M., Dulaney, T. R., Gresham, M. I., & Tam, H. 2008a, [[arXiv:0812.1049](#)]
- Carroll, S. M., Tseng, C.-Y., & Wise, M. B. 2008b, [[arXiv:0811.1086](#)]
- Chang, S., Kleban, M., & Levi, T. S. 2008, [[arXiv:0810.5128](#)]
- Copi, C. J., Huterer, D., Schwarz, D. J., & Starkman, G. D. 2006, *MNRAS*, 367, 79
- Cruz, M., Martínez-González, E., Vielva, P., & Cayón, L. 2005, *MNRAS*, 356, 29
- Cruz, M., Tucci, M., Martínez-González, E., & Vielva, P. 2006, *MNRAS*, 369, 57
- de Oliveira-Costa, A., Tegmark, M., Zaldarriaga, M., & Hamilton, A. 2004, *Phys. Rev. D*, 69, 063516
- Erickcek, A. L., Carroll, S. M., & Kamionkowski, M. 2008a, *Phys. Rev. D*, 78, 083012
- Erickcek, A. L., Kamionkowski, M., & Carroll, S. M. 2008b, *Phys. Rev. D*, 78, 123520
- Eriksen, H. K., Hansen, F. K., Banday, A. J., Górski, K. M., & Lilje, P. B. 2004a, *ApJ*, 605, 14
- Eriksen, H. K., Banday, A. J., Górski, K. M., & Lilje, P. B. 2004b, *ApJ*, 612, 633
- Eriksen, H. K., Novikov, D. I., Lilje, P. B., Banday, A. J., & Górski, K. M. 2004c, *ApJ*, 612, 64
- Eriksen, H. K., Banday, A. J., Górski, K. M., & Lilje, P. B. 2005, *ApJ*, 622, 58
- Eriksen, H. K., et al. 2007a, *ApJ*, 656, 641
- Eriksen, H. K., Banday, A. J., Górski, K. M., Hansen, F. K., & Lilje, P. B. 2007b, *ApJ*, 660, L81
- Finkbeiner, D.P., Davis, M., & Schlegel, D.J. 1999, *ApJ*, 524, 867
- Finkbeiner, D. P. 2003, *ApJS*, 146, 407
- Gold, B., et al. 2009, *ApJS*, 180, 265
- Gordon, C., Hu, W., Huterer, D., & Crawford, T. 2005, *Phys. Rev. D*, 72, 103002
- Gordon, C. 2007, *ApJ*, 656, 636
- Górski, K. M., Hivon, E., Banday, A. J., Wandelt, B. D., Hansen, F. K., Reinecke, M., Bartelman, M. 2005, *ApJ*, 622, 759
- Groeneboom, N. E., & Eriksen, H. K. 2009, *ApJ*, 690, 1807
- Emir Gümrükçüoğlu E., A., Contaldi, C. R., & Peloso, M. 2007, *JCAP*, 11, 5
- Guth, A. H. 1981, *Phys. Rev. D*, 347
- Hansen, F. K., Banday, A. J., & Górski, K. M. 2004, *MNRAS*, 354, 641
- Hansen, F. K., Banday, A. J., Gorski, K. M., Eriksen, H. K., & Lilje, P. B. 2008, *ApJ*, submitted, [[arXiv:0812.3795](#)]
- Haslam, C. G. T., Salter, C. J., Stoffel, H., & Wilson, W. 1982, *A&AS*, 47, 1
- Himmetoğlu, B., Contaldi, C. R., & Peloso, M. 2008a, [[arXiv:0809.2779](#)]
- Himmetoğlu, B., Contaldi, C. R., & Peloso, M. 2008b, [[arXiv:0812.1231](#)]
- Hinshaw, G., et al. 2006, *ApJ*, submitted, [[astro-ph/0603451](#)]
- Jaffe, T. R., Banday, A. J., Eriksen, H. K., Górski, K. M., & Hansen, F. K. 2005, *ApJ*, 629, L1
- Jaffe, T. R., Banday, A. J., Eriksen, H. K., Górski, K. M., & Hansen, F. K. 2006, *A&A*, 460, 393
- Jeffreys, H. 1961, “Theory of probability”, 3rd edition, (OUP, Oxford)

- Kahniashvili, T., Lavrelashvili, G., & Ratra, B. 2008, Phys. Rev. D, 78, 063012
- Kanno, S., Kimura, M., Soda, J., & Yokoyama, S. 2008, JCAP, 8, 34
- Koivisto, T., & Mota, D. F. 2008a, JCAP, 8, 21
- Koivisto, T., & Mota, D. F. 2008b, ApJ, 679, 1
- Komatsu, E., et al. 2009, ApJS, 180, 330
- Linde, A. D., 1982, Phys. Lett. B 108, 389
- Linde, A. D., 1983, Phys. Lett. B 155, 295
- Linde, A. D., 1994, Phys. Rev. D49, 748
- Martínez-González, E., Cruz, M., Cayón, L., & Vielva, P. 2006, New Astronomy Review, 50, 875
- McEwen, J. D., Hobson, M. P., Lasenby, A. N., & Mortlock, D. J. 2008, MNRAS, 388, 659
- Muhkanov, V. F., Chibishov, G. V., Pis'mah Zh. 1981, Exsp. Teor. Fiz. 33, 549
- Mukherjee, P., Parkinson, D., & Liddle, A. R. 2006, ApJ, 638, L51
- Pereira, T. S., Pitrou, C., & Uzan, J.-P. 2007, JCAP, 9, 6
- Pitrou, C., Pereira, T. S., & Uzan, J.-P. 2008, JCAP, 4, 4
- Pullen, A. R., & Kamionkowski, M. 2007, Phys. Rev. D, 76, 103529
- Räth, C., Schuecker, P., & Banday, A. J. 2007, MNRAS, 380, 466
- Ruhl, J. E., 2003, ApJ599, 786
- Runyan, M. C., 2003, ApJ, J. Suppl. Ser. 149, 265
- Scott, P. F., 2003, MNRAS341
- Skilling, J. 2004, in AIP Conf. Proc. 735, Bayesian Inference and Maximum Entropy Methods in Science and Engineering. ed. R. Fischer, R. Preuss, & U. von Toussaint (Melville: AIP), 395
- Smoot, G. F., 1992, ApJ396, L1
- Starobinsky, A. A., 1980, Phys. Lett. B, 91, 99
- Starobinsky, A. A., 1982, Phys. Lett. B 117, 175
- Vielva, P., Martínez-González, E., Barreiro, R. B., Sanz, J. L., & Cayón, L. 2004, ApJ, 609, 22
- Watanabe, M.-a., Kanno, S., & Soda, J. 2009, [arXiv:0902.2833]
- Yadav, A. P. S., & Wandelt, B. D. 2008, Phys. Rev. D, 100, 181301
- Yokoyama, S., & Soda, J. 2008, JCAP, 8, 5